Lasers in Manufacturing Conference 2017

Marangoni force and numerical instability when modelling keyhole laser welding

J. Svenungsson[a,*], I. Choquet[a], A. Kaplan[b]

[a]*University West, Sweden, josefine.svenungsson@hv.se*
[b]*Luleå University of Technology, Sweden*

Abstract

This work is a first step in a study aiming at predicting defects such as porosity in keyhole laser welded titanium alloy Ti6Al4V in order to understand their cause and improve the process. For this a multi-phase thermo-fluid model for keyhole laser welding was implemented in the open source software OpenFOAM®. In order to model porosity, free surface tracking and the gas phase are included in the model. Surface tracking is done with a Volume of Fluid method improved to reduce numerical diffusivity. Solid, liquid and gas phases are taken into account and vaporization is modelled through its effect on pressure and enthalpy. This paper treats the validation of the model by comparing the model to published numerical test cases. A test case revealed stability problems related to the implementation of Marangoni force. It was shown that the implementation method used for the Marangoni force can lead to numerical instabilities. This unphysical behavior, which could affect the prediction of pore formation, might not be detected by the usual weld geometry validation test case. This resulted in improvement of the numerical model. Another test case is a comparison between different surface tracking methods and was done in order to evaluate the model ability to capture formation of porosity, vapor bubbles. The results show a significant difference between VOF and CLSVOF.

Keywords: process simulation; CFD; keyhole laser welding; OpenFOAM; validation; Marangoni convection

* Corresponding author.
E-mail address: josefine.svenungsson@hv.se .

1. Introduction

Keyhole laser welding is a joining process characterized by a low heat input and large welding speed, generating welds with a narrow bead and high depth to width ratio. The main defects in keyhole laser welding is humping, spatter and porosity; another defect of importance is hot cracking. The focus in this study is on formation of porosity and the detection of pores with a minimum size of 10 µm. For this, a thermo-fluid model (a one fluid model) which includes solid and liquid metal phases, and the shielding gas vapor phase is developed and implemented. The solid/liquid transition region is described with the mushy zone approach. The deformation of the liquid/vapor interface is tracked with a VOF (Volume of Fluid) method modified to reduce numerical diffusivity. An additional convective term that depend on the compression velocity, U_r=U_l-U_g, which is the relative velocity between the two phases, is calculated in the volume fraction equation. The additional term is active only in a region close to the interface. It increases the local gradient of the volume fraction on the interface, thus compressing it, reducing the diffusivity and keeping its boundedness, (Saldi (2009) and Rusche (2002)).

The temperature dependence of the thermodynamic and transport properties in the solid, liquid and vapor phases is neglected. The model does not yet include a ray tracing method. It is thus limited to low to moderate welding speed (not exceeding 1m/min) for which keyhole bending remains negligible.

The conservation equations governing the metal volume fraction, α, the density, ρ, the momentum, $\rho\vec{u}$, and the enthalpy, ρh, are respectively written as:

$$\partial_t \alpha + \nabla\cdot(\alpha\vec{u}) + \nabla\cdot[(1-\alpha)\alpha\vec{u}_r] = \nabla\cdot(\alpha\vec{u}_r) + \dot{\alpha} \qquad \text{with} \qquad 0 \le \alpha \le 1$$

$$\partial_t \rho + \nabla\cdot[\rho\vec{u}] = 0,$$

$$\partial_t(\rho\vec{u}) + \nabla\cdot[\rho\vec{u}\vec{u}] = F_s + F_v,$$

$$\partial_t(\rho h) + \nabla\cdot[\rho h\vec{u}] = \nabla\cdot(k\nabla T) - \alpha_1 S_h + Q_{hs} - Q_{vap}$$

The continuity equation is used together with the momentum equation to derive the pressure equation.

The forces acting on the melt pool are divided into surface forces and volumetric forces, denoted by F_s and F_v respectively. Surface tension and Marangoni force are handled as surface forces and are multiplied by a damping factor, which is redistributing the surface forces to the denser phase. Brackbill et al. (1992) previously used this kind of factor in order to solve problems with high flow accelerations in the less dense fluid phase.

Buoyancy, gravitational force and pressure are accounted for in the volumetric forces, F_v.

$$F_s = \nabla\cdot(\mu_f\nabla U) + \left(\sigma + \frac{\partial\sigma}{\partial T}(\nabla T - n(n\cdot\nabla T))\right)\cdot|\nabla\alpha|\cdot\frac{2\rho}{(\rho_{l1}f_l + (1-f_l)\rho_{s1} + \rho_2)} - A\vec{u}$$

$$F_v = \rho\beta_1(T - T_{ref})\cdot g - g\cdot\nabla p - \nabla p + \rho g$$

The recoil pressure, P_v, given the Clausius-Clapeyron equation

$$P_v = P_0 exp\left[(m_1 H_v/k_B)\cdot\left(\frac{T-T_v}{T\cdot T_v}\right)\right]$$

where m_1 denote the molecular mass of phase 1, H_v is the latent heat of evaporation, k_B the Stefan Boltzmann constant and T_v the vaporization temperature. In order to account for vaporization due to the

heat source the term $Q_{vap} = \dot{m}H_v$ is included in the energy equation. Where the evaporation rate, or vapor mass source term, $\dot{m}$, is the Langmuir equation as stated in Hirano (2011) and given as:

$$\dot{m} = \alpha_1 \alpha_2 P_v \cdot \sqrt{\frac{m_1}{2\pi k_B T}} \cdot \frac{1}{L}$$

The term $A\vec{u}$ is the Darcy damping factor that depend on the liquid fraction and act as a sink term in the dense phase, forcing the velocity field in the solid phase to zero, to avoid unphysical behavior. The Darcy damping factor is written as:

$$A = \frac{K(1 - f_L^2)}{f_L^3 + B}$$

where K is a large constant, $1e^6$, and B, $1e^{-3}$, is a small constant used to avoid division by zero. f_L is the liquid fraction as described by Rösler and Brüggemann (2011):

$$f_L = 0.5 \cdot erf\left(\frac{4(T - T_m)}{(T_l - T_s)}\right) + 0.5$$

The forces in F_v are the buoyancy and gravitational forces as well as the pressure terms.

S_h , in the energy equation is a source term for latent heat, previously described by Rösler and Brüggemann (2011) and written as:

$$S_h = -\rho h_{melt} \frac{4 \cdot exp\left(\frac{4(T - T_m)}{T_l - T_s}\right)^2}{\sqrt{\pi} \cdot (T_l - T_s)} \cdot \left(\frac{\partial T}{\partial t} + U \cdot \nabla T\right)$$

with h_{melt} latent heat of melting and T_m, T_l and T_s are the melting, liquidus and solidus temperatures. The convective term of the latent heat is included.

Density, viscosity, specific heat and thermal conductivity are assumed constant in each phase and the mixture (local) property is defined as:

$$\rho = \alpha_1\big(f_L \rho_{l1}(1 - f_L)\big)\rho_{s1} + \alpha_2 \rho_2,$$

$$\mu = \alpha_1 f_L \mu_1 + \alpha_2 \mu_2,$$

$$C_p = \alpha_1\big(f_L \rho_{l1}(1 - f_L)\big)\rho_{s1} + \alpha_2 \rho_2,$$

$$k = \alpha_1\big(f_L k_{l1} + (1 - f_L)\big)k_{s1} + (1 - \alpha_1)k_2$$

The laser beam is represented by an adaptive volumetric heat source in 3D with a Gaussian distribution, Xu et al. (2011).

The numerical model was implemented in the open source software OpenFOAM® based on the multi-phase solver interFoam which applies to two incompressible, isothermal and immiscible fluids and uses a VOF phase-fraction based interface capturing approach.

The problem with the existing model is the evaporation phase change. Since there is no analytical solutions and no simple numerical test cases isolating specific physical aspects available, test cases for related physical phenomenon has to be used in order to validate the model.

Several models of keyhole laser welding combining beam-matter interaction and fluid flow have been developed, starting from the first model by Ki et al. (2001). A detailed review of the existing numerical models, using CFD techniques, for keyhole laser welding is given in Svenungsson et al. (2015). The variety of the models' assumptions and limitations show that this field is still under development.

The purpose of the study presented here is to, by existing numerical test cases, test specific parts of the implemented model. The validation step consists of investigating the influence of Marangoni force on stability in numerical modeling, the interface tracking method's ability to handle large interface deformations and the evaporation phase change model by the use of three different test cases. Due to the lack of analytical solutions it is also common to use macroscopic measurements with cross-sectional images and temperature measurements in order to validate numerical models. Marangoni convection in keyhole laser welding modelling is important since it drives heat and mass transfer in the melt pool, Zhou et al. (2006), Cho et al. (2009), and the size and shape of the melt pool, Xu et al. (2007), Amberg et al. (2008), Suthakar (2012), Wei et al. (2012).

Previous studies show that 2D models are not sufficient in order to capture the important characteristics in keyhole laser welding, Xiao-Hu et al. (2002

Limmaneevichitr et al. (2000) performed experimental studies with the aim of investigating Marangoni convection in arc weld pools using a defocused CO_2-laser heat source. By flow visualization and a laser-light cut technique, they study the Marangoni convection in transparent melt pools of NaNo3. The effect of beam diameter and power on the flow pattern is investigated by measuring the beam diameter of the heat source and the surface temperature in the melt pool. Their findings are in line with previous studies showing that Marangoni convection dominates over gravity induced buoyancy in the melt pool.

Other numerical models with focus on Marangoni convection, but not welding, is for example the study by Peng et al. (2000), which investigate melting in laser-assisted processes. By first evaluating the time for melting, generating an initial melt pool and then include fluid flow they calculate the velocity and temperature fields of the molten pool. Their study consists of three cases with different initial melt pool sizes and aim at investigating the Marangoni convection effect in the melt pool. The observations made are that Marangoni convection plays a much more significant role than natural convection in the melt pool flow, thus it is important to include in numerical models of laser-assisted processes. It is also concluded that the Marangoni convection influences the temperature distribution and fluid flow, thus affecting the shape of the weld pool.

Some previous studies, Nas et al. (2000), Sasmal (1994), focused on investigating the Marangoni convection in other applications than laser welding for example in a cavity. Tan et al. (2006) developed a test case for validating the Marangoni driven free surface flow for models aiming at studying solidification and crystal growth. The test case is described in the next section of this paper.

Saldi et al. (2009) published a study on the Marangoni driven flows in melt pools generated during laser spot welding of stainless steel. They performed numerical and experimental observations in order to study the influence of surface active elements on the weld pool flow. Their observations showed that surface tension and surface tension gradient affect the direction of the Marangoni shear stress, which affect the flow direction in the weld pool.

Some models assume that Marangoni convection is negligible in the keyhole, but when modelling the keyhole laser welding process the whole melt pool is of interest and as previous studies show, Marangoni

convection influences the melt pool flow and the solidification process. The Marangoni convection is affected by the gas flow, for example the shielding gas, thus, it is important to include in the numerical model of keyhole laser welding. An increased understanding of the physics influencing the weld pool flow help to increase the weld quality, to better control the weld shape and optimize process parameters.

This study is the first step in developing and implementing a numerical model in OpenFOAM, with the aim of predicting porosity formation in keyhole laser welded materials. The effect of Marangoni convection on stability is analyzed as well as the representation of the deforming liquid-vapor interface.

The remaining part of the paper describes three different numerical test cases and their results followed by conclusions and future work.

2. Test Case – Marangoni driven flow

In the first test case, the Marangoni convection driven flow is studied. The test case was first published by Tan et al. (2006) and more recently by Z. Saldi (2012). Marangoni convection, which is the thermocapillary force, appear due to surface tension gradients. Combined with phase change and surface deformation, the thermocapillary force represents complex physical processes, such as welding. Surface tension gradients caused by temperature variations on the melt surface induce a flow from low to high surface tension regions. The Marangoni convection influences the crystal growth in the solid-liquid interface and thus affect the weld shape, as described previously in the Introduction. The test case employed here, represents the solid-liquid phase change of pure bismuth in a 2D container. The container is filled with pure bismuth and above the bismuth, argon gas. The left wall of the container is hot and the right wall is cold, generating a linear temperature gradient, which induces a thermocapillary convective flow. Microgravity condition, with g = $4.145 \cdot 10^{-5}$ m/s^2, is applied in order to emphasis the effect of Marangoni force, under normal gravitational condition, the buoyancy effects usually dominate and Marangoni is less significant.

Dimensionless numbers describing the solid-liquid phase change and the convection in the melt are used in the test case. From these the surface tension coefficient and surface tension gradient are calculated. The dimensionless numbers are: the Marangoni number, $Ma = \gamma \Delta T d/\alpha\mu = 244$ the Capillary number, $Ca = \gamma \Delta T/\sigma = 0.0022$, and the Bond number, $Bo = \rho g d^2/\sigma = 0.000188$. Rayleigh, $Ra = \beta g \Delta T d^3/\nu\alpha = 0.031$, Prandtl number, $Pr = C_p \mu k = 0.019$, and the Stefan number, $Ste = C_p \Delta T/L_f = 0.033$ are also used.

In the equations $\gamma = -d\sigma/dT$ is the surface tension gradient. ΔT is the temperature difference between hot and cold wall, d is the initial melt depth ,α is the thermal diffusivity, μ is the dynamic viscosity, ν is the kinematic viscosity, σ is the surface tension coefficient, C_p is the specific heat, ρ is the density, g is the gravity and L_f is the latent heat of fusion.

The calculation domain is a 2D container and the boundary conditions for solid and gas are the same. The velocity condition used is a no-slip condition applied on all sides of the domain. The temperature, initially linearly distributed on top and bottom boundary are set to a fixed temperature according to the values given in Tan et al. (2006). The pressure conditions applied to all boundaries is a Neumann condition (zero gradient). OpenFOAM uses a pressure term called p-rgh, which is not the real pressure. P-rgh changes throughout the domain due to density changes. Thus, OpenFOAM requires BC's or initial conditions for both p and p-rgh. A reference point and reference value for the pressure needs to be defined and is, in this case, set in the lower right part of the domain where no phase change is expected to occur. The value added from ρgh is small compared to the atmospheric pressure, 100 000 Pa, since the calculation domain is only 5 mm in z-direction. In the initialization phase, the same boundary condition for p and p-rgh can therefore be applied.

In order to decrease the computational time, a steady state conduction solution is used to set the initial temperature distribution. Then the solver, described earlier in this section, is used to calculate the Marangoni driven flow. For pressure-velocity coupling, the iterative PIMPLE algorithm is utilized. A fixed time step of $\Delta t = 1e^{-5}$ is used.

For the test case, a non-uniform mesh with a finer grid closer to the free surface is defined. The mesh corresponds to the mesh used by Saldi (2012) and Tan et al. (2006) with a mesh size of 140 x 67 cells. A mesh independency study was presented by Tan et al. (2006) showing that the mesh with 110 x 60 cells compared

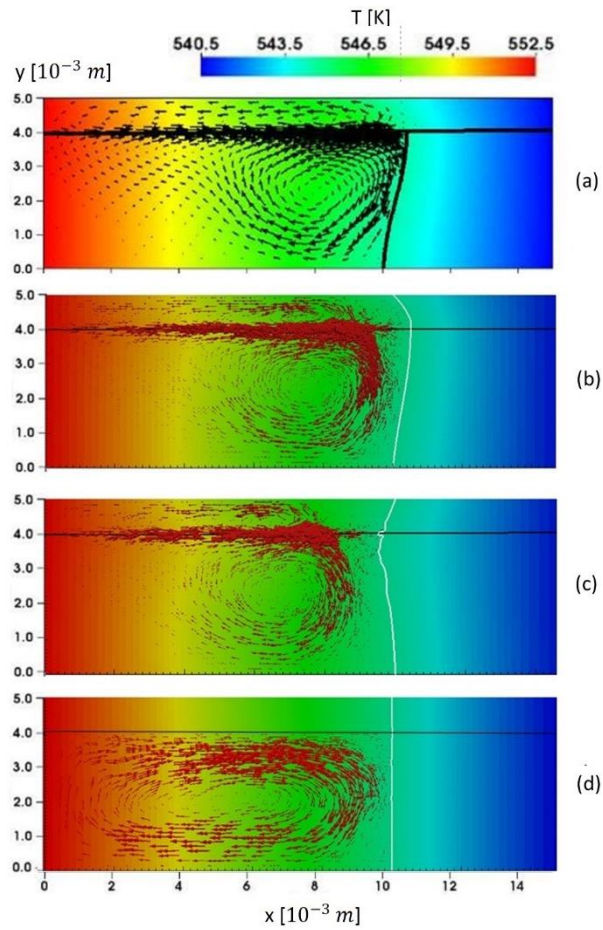

Fig. 1. a) Saldi results, Saldi (2012), b) result from the implemented solver, c) with a different implementation of Marangoni force and d) with convective latent heat.

to 150 x 80 cells only make a 0.6% difference on the predicted position of the crystal interface. Thus, a mesh independency study has not been performed here.

The test case used to validate the numerical model's ability to predict the Marangoni driven flow showed a good agreement with previously published results, Fig 1a and b. However, the test case (Tan et al. (2006)

and Saldi (2012)) does not account for the convective term of the latent heat and by comparing the results from calculation with (Fig 1c) and without (Fig 1b) the convective latent heat it is shown that the convective term affects the Marangoni convection and temperature distribution. The horizontal black line is the interface between gas and bismuth while the white vertical line is the liquid fraction, $f_L = 0.5$, also denoted melting front.

It was also found that the way the Marangoni convection term is implemented significantly affect the numerical stability and solidification front. The Marangoni convection can be implemented as a surface force or as a volume force and the choice of implementation method makes a difference on the temperature distribution and melting front. A study was conducted on the implementation of Marangoni convention. A force can be either a surface or a volume force and in OpenFOAM the operation reconstruct is used in order to change between a volume field and a surface field. With Marangoni convection implemented as a surface force and the surface normal is the normal of the cell instead of the interface normal it might lead to a wrong direction of the Marangoni driven flow. Figure 1 d show the result from the test case, described above, when Marangoni is implemented on LHS vs RHS of the momentum equation. Since the implementation has a significant influence on the resulting flow, heat transfer and solidification front and no validation study is available this has to be further investigated.

3. Test case 2 VOF, OpenFOAM VOF and CLSVOF with rising bubble

The second test case is the rising of a circular gas bubble in a liquid. The gas bubble, with diameter d=0.5 m, is placed in the lower part of a rectangular domain, 1 x 1.7 m^2, filled with a stationary liquid. A grid size of 128 x 218 cells is used. The test case is used with mass conserving Level Set, MCLS, VOF and a Coupled Level Set and Volume of Fluid, CLSVOF, method. Ningegowda and Premachandran (2014) further describe the test case. The CLSVOF method is a combination of the benefits from both VOF and LS and gives a more accurate resolution of two-phase flows.

The rising bubble test case results show that the rising velocity is different depending on which interface tracking method is used. Figure 2 show the comparison of VOF, OpenFOAM implementation of VOF and CLSVOF. The difference between MCLS and OpenFOAM VOF representation of the downward pointing deformation of the bubble is increasing with time. It can be seen from Fig. 2 that OpenFOAM does nog accurately capture the interface in the regions with high surface tension and large curvature.

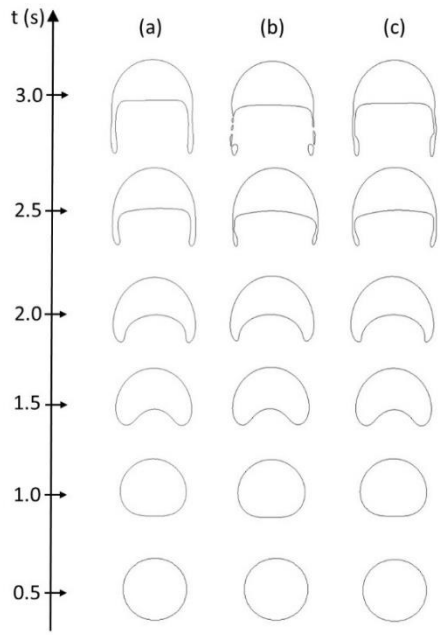

Fig. 2. Comparison of MCLS, OpenFOAM VOF and CLSVOF

4. Test case 3 Evaporation model

The physical phenomena of a liquid drop in contact with a surface hotter than the boiling point of the liquid generates a protecting layer of vapor around the drop. The increased pressure between the drop and the surface, due to evaporation, act as a lifting or repulsive force keeping the drop hovering over the surface. This phenomenon is called the Leidenfrost effect. Test case 3 presented here consists of a water droplet falling towards a hot surface. The surrounding gas is water vapor. An axi-symmetrical wedge of 2 mm height and 1 mm radii is meshed with a non-uniform mesh consisting of denser mesh closer to the hot surface and the symmetry axis. An adjustable time step with minimum $\Delta t = 1e^{-6}$ is used. The droplet is initially at a distance 1.25 mm above the hot surface and falls when the calculation is initiated. It is partly deformed when hitting the surface but due to the Leidenfrost phenomenon, combined with a low Weber number, it does not splash but rather bounces on the surface. The test case presented and further described by Kunkelmann (2011) is used to validate the evaporation phase change model.

The difference between OpenFOAM-2.2 original volume fraction equation and the volume fraction equation by Kunkelmann lies in the representation of evaporation phase change. For low Weber number and low impact velocity droplet bouncing is expected. In the test case presented here the dimensionless Weber number, $\boldsymbol{We} = \frac{\rho v^2 D}{\sigma}$, is 2.55 and the velocity of the impacting droplet is only due to gravity. Figure 3 show a comparison between simulation results, of the water drop reaching the hot surface and bouncing back, and experimental observations Lin (2012).

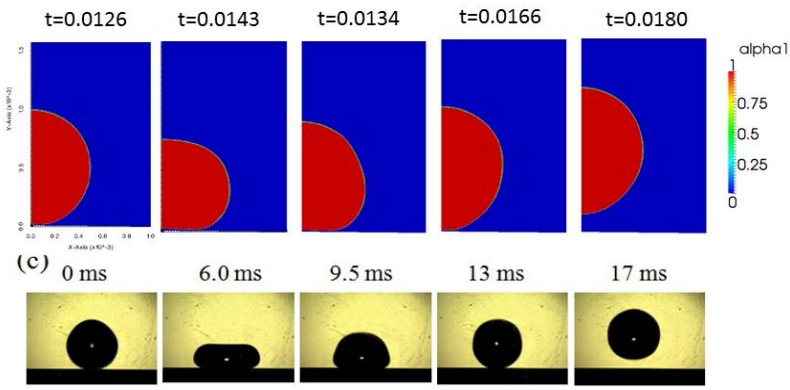

Figure 10. Snapshots of free fall droplets released from various surfaces at rebounding temperature (T_r):(a) on the oxidized silicon at T_r=165°C,(b) on the vertical CNTs surface at T_r=247°C, (c)on the curved CNTs surface at T_r=257°C .

Fig. 3. Top images show simulation results of a water droplet bouncing at hot surface. Lower images show experimental results obtained by C. Lin (2012).

5. Conclusions and future work

By the use of three numerical test cases, different parts of the model is be validated. With the first test case it was found that the way the Marangoni force is implemented affects the numerical stability of the calculation and affects also the flow pattern and thus the temperature distribution. The same test case was used to study the influence of convective latent heat since some previous studies neglect the convective latent heat. When neglecting the convective latent heat the results were in good agreement with the results presented in Saldi (2012) and Tan et al. (2006). But it was shown that when the convective latent heat was included it contributed significantly to the flow and temperature distribution and thus cannot be neglected in keyhole laser welding modelling.

For the purpose of studying pore formation in laser welding the evaporation phase and the representation of gas bubble shape and movement is of high importance. For this test case 2 and 3 was used to validate those specific parts of the model. Test case 2 showed a significant difference between Level Set, OpenFOAM VOF and CLSVOF in handling large curvatures in the interface and in regions with high surface tension. CLSVOF proved to give a more accurate solution compared to OpenFOAM VOF. This might lead to prediction of porosity in the solidified material where the pores in reality should have reached the surface prior to solidification.

Test case 3 was used to validate the evaporation part of the model. Fig 3 show a good agreement between simulation results of a water droplet compared to experimental observations.

Acknowledgements

This work was supported by VINNOVA, programme NFFP6, project no. 2013-01139, in collaboration with GKN Aerospace Engine Systems. These supports are gratefully acknowledged.

References

Amberg, G., Do-Quang, M., 2008. Thermocapillary convection and phase change in welding. Int. J. of Numerical Methods for Heat & Fluid Flow 18, 378-386.

Brackbill, J.U., Kothe, D. B., Zemach, C., 1992. A continuum method for modeling surface tension. J. of Comp. Physics, 100, 335-354.

Cho, J.H., Farson, D.F., Milewski, J.O., Hollis, K.J., 2009. Weld pool flows during initial stages of keyhole formation in laser welding. Journal of Physics D: Applied Physics 42.

Hirano, K., Fabbro, R., Muller, M., 2011. Experimental determination of temperature threshold for melt surface deformation during laser interaction on iron at atmospheric pressure. J. Phys. D. Appl. Phys., 44, 435402.

Ki, H., Mohanty, P.S., Mazumder, J., 2001. Modeling of high density laser material interaction using fast level set method. Journal of Physics D: Applied Physics 34(3), 364-372.

Kunkelmann, C., PhD-thesis, Numerical modelling and investigation of boiling phenomena, Darmstadt Germany, May, 2011.

Limmanevichitr, C., Kou, S., 2000. Experiments to simulate effect of Marangoni convection on weld pool shape. Welding Journal New York, 79, 231.

Limmanevichitr, C., Kou, S., 2000. Visualization of Marangoni convection in simulated weld pools. Welding Journal New York, 7 9, 126.

Nas, S., Tryggvason, G., 2003. Thermocapillary interaction of two bubbles or drops. Int. J. of Multiphase flow, 29, 1117-1135.

Ningegowda, B.M., Premachandran, B., 2014. A Coupled Level Set and Volume of Fluid method with multi-directional advection algorithms for two-phase flows with and without phase change. Int. Journal of Heat and Mass Transfer, 79, 532-550.

Rusche, H., PhD-thesis, Computational Fluid Dynamics of Dispersed Two-Phase Flows at High Phase Fractions. University of London, Dec. 2002.

Rösler, F., Brüggemann, D., 2011. Shell-and-tube type latent heat thermal energy storage: numerical analysis and comparison with experiments. Journal of Heat and Mass Transfer, 47, 1027-1033.

Saldi, Z. S., Zhao, C., Kenjeres, S., Richardson, I.M., Kleijn, C.R. Numerical and experimental investigations of Marangoni driven flow reversals in liquid steel welding pools.

Saldi Z., PhD-thesis, Marangoni driven free surface flows in liquid weld pools, Delft, Netherlands, Dec. 2012.

Sasmal, G.P., Hochstein, J.I., 1994. Marangoni convection with a curved and deforming free surface in a cavity. Journal of fluids engineering, 116, 577-582.

Suthakar, T., Balasubramanian, K.R., Sankaranarayanasamy, K., 2012. Studies on weld shape formation and Marangoni convection in Nd:YAG laser welding. Int. J. Mechatronics and Manufacturing Systems, 5.

Tan, L.H., Leong, S.S., Leonardi, E., Barber, T.J., 2006. A numerical study of solid-liquid phase change with Marangoni effects using a multiphase approach. Progress in Computational Fluid Dynamics, 6, 304-313.

Tan, W. Bailey, N.S., Shin, Y.C., 2013. Investigation of keyhole plume and molten pool based on a three-dimensional dynamic model with sharp interface formulation. J. Phys. D. Appl. Phys., 46.

Wei, P.S., Liu, H.J., Lin, C.I., 2012. Scaling weld or melt pool shape induced by thermocapillary convection. Int. Journal of Heat and Mass Transfer, 55, 2328-2337.

Xiao-Hu, Y., Xi, C., 2002. Importance of Marangoni convection in laser full-penetration welding. Chinese physics letters, 19, 788.

Xu, Y.L., Dong, Z.B., Wei, Y.H., Yang, C.L., 2007. Marangoni convection and weld shape variation in A_TIG welding process. Theoretical and Applied Fracture Mechanics 48, 178-186.

Xu, G.X., Wu, C.S., Qin, G.L., Wang, X.Y., Lin, S.Y., 2011. Adaptive volumetric heat source models for laser beam and laser + pulsed GMAW hybrid welding processes. Int. Journal of Advanced Manufacturing Technology, 57, 245-255.